Journal of Orthopaedic Translation (2014) 2, 35—42

Available online at www.sciencedirect.com

ScienceDirect

journal homepage: http://ees.elsevier.com/jot

ORIGINAL ARTICLE

Enhanced osteointegration of medical titanium implant with surface modifications in micro/nanoscale structures

Liwen Lin [a,b], Hui Wang [a], Ming Ni [c], Yunfeng Rui [c], Tian-Yuan Cheng [c], Cheng-Kung Cheng [d,e], Xiaohua Pan [e], Gang Li [c,f,g,**], Changjian Lin [a,b,*]

[a] *State Key Laboratory of Physical Chemistry of Solid Surfaces and College of Chemistry and Chemical Engineering, Xiamen University, Xiamen, Fujian 361005, China*
[b] *Beijing Medical Implant Engineering Research Center, Beijing Naton Technology Group, Beijing, China*
[c] *Department of Orthopaedics and Traumatology, Faculty of Medicine, The Chinese University of Hong Kong, Hong Kong, China*
[d] *International Research Center for Implantable and Interventional Medical Devices, Beihang University, Beijing, China*
[e] *Department of Orthopaedics and Traumatology, Shenzhen City People's Hospital, Luohu Distract, Shenzhen, China*
[f] *Program of Stem Cell and Regeneration, School of Biomedical Science and Li Ka Shing Institute of Health Sciences, Faculty of Medicine, The Chinese University of Hong Kong, Hong Kong, China*
[g] *Lui Che Woo Institute of Innovative Medicine, Faculty of Medicine, The Chinese University of Hong Kong, Hong Kong, China*

Received 15 June 2013; received in revised form 11 August 2013; accepted 19 August 2013
Available online 14 December 2013

KEYWORDS
Electrochemistry;
Osteointegration;
Roughness;
Surface modification;
Titanium

Summary Biomimetic design and substrate-based surface modification of medical implants will help to improve the integration of tissue to its material interfaces. Surface energy, composition, roughness, and topography all influence the biological responses of the implants, such as protein adsorption and cell adhesion, proliferation and differentiation. In the current study, different surface structures of Ti implants were constructed using facile surface techniques to create various micro-, nano-, and nano/micro composite scale topography. We have fabricated three types of hierarchical structures of TiO_2 coating on Ti implants, including nanotube

* Corresponding author. State Key Laboratory of Physical Chemistry of Solid Surfaces and College of Chemistry and Chemical Engineering, Xiamen University, Xiamen, Fujian 361005, China. Tel.: +86 592 2189354; fax: +86 592 2186657.
** Corresponding author. Department of Orthopaedics and Traumatology, Faculty of Medicine, The Chinese University Hong Kong, Prince of Wales Hospital, Shatin, Hong Kong, China.
E-mail addresses: gangli@cuhk.edu.hk (G. Li), cjlin@xmu.edu.cn (C. Lin).

http://dx.doi.org/10.1016/j.jot.2013.08.001

structure, nano sponge-like structure, and nano/micro nest-like structure. The osteointegration and biomechanical performance of the coated Ti screws were evaluated by histology and removal of torque force test *in vivo*. We found that the nano/micro nest-like and nanotube structured surface possessed better osteointegration ability. It indicated that the alkaline hydrothermally treated Ti substrate was the best for bone-implant integration in terms of all *in vitro* and *in vivo* testing parameters. The alkaline hydrothermally treated surface displayed a hydrophilic (contact angle value 5.92 $\pm$ 1.2), higher roughness (Ra value 911.3 $\pm$ 33.8 nm), higher specific surface area (8.26 $\pm$ 1.051 m^2/g), and greater apatite inductivity. The electrochemical surface modification may become a powerful approach to enhance metal implant to bone integration in orthopaedic applications.

Introduction

Ti-based materials have been widely used in orthopaedics and dental surgery as implants because of their strong mechanical properties and good chemical stability and biocompatibility [1]. To enhance osteogenetic differentiation and osteointegration of implants, various treatments have been developed to modify the surface chemistry, physical properties, and topography; approaches include machining/micromachining, sandblasting, acid etching, electropolishing, anodic oxidation, and plasma spraying [2—5]. These techniques mainly alter the surface parameters, leading to enhancement of cell attachment to the implant surfaces. In the assays, cells grow and integrate better on the modified surfaces by producing more extracellular matrix components, including cell adhesive proteins or type I collagen and fibronectin [6,7]. However, the results from *in vitro* studies may be different from the *in vivo* situation. Osteointegration is the direct anchorage of an implant by the formation of bony tissues around the implant without the growth of fibrous tissues at the bone—implant interfaces [8], which is influenced by a wide range of factors including anatomical location, implant size and design, surgical procedure, loading effects, biological fluids, age, sex, and particularly, the implant surface characteristics [9]. Torque removal force has been used as a biomechanical measure of anchorage or osteointegration in which the greater force required to remove implants may be interpreted as an increase in the strength of osteointegration.

Surface composition, topography, wettability, roughness, and surface electrical charge are key parameters in determining implant—tissue interaction and osteointegration [10—12]. Roughness of the implant surfaces usually results in cellular adherence through guiding the cytoskeletal assembly and membrane receptor organization and accelerating the adsorption of fibronectin and albumin [13,14]. A positive relationship has been found between bone-to-implant contact and implant surface roughness [15]. Sandblasted and acid-etched surface implants are nowadays commercially available as dental implants with microscale average roughness [16]. Gittens et al [17] introduced nanoscale structures with micro/submicroscale roughness without chemical composition and contact angles modification, and improved the osteoblast differentiation and local growth factors production. Zinger et al [18] reported that with surface modification of Ti material with hierarchical surface roughness, osteoblasts responded differently towards nano-, micro-, or nano/micro topography. The pattern, size, and distribution of peaks and valleys that compose the surface roughness are also important factors influencing osteointegration.

The optimal surface roughness for metal implant osteointegration has not yet been well defined. A thick surface oxide layer is desirable because of its ability for hydrocarbon adsorption [9]. Medical devices might also benefit from hydrophilic surface treatment to reduce interfacial inflammatory responses and promote bony ingrowth [1]. In this study, different Ti implant surface structures were constructed using facile surface techniques to create various micro-, nano-, and nano/micro composite scale topographies, including nanotubular structure, nano sponge-like structure, and nano/micro nest-like structure. The surface was characterized by various physicochemical methods, and the bioactivity and osteointegration were investigated through *in vitro* and *in vivo* evaluations.

Materials and methods

Preparation of coatings

Ti foils (Baoji Titanium Industry Co. Ltd., China) of 0.1-mm in thickness and 99.5% purity were used. Prior to the different treatments, the Ti sheets (10 mm $\times$ 10 mm) were degreased in an ultrasonic bath in acetone, anhydrous ethanol, and deionised (DI) water successively, followed by rinsing with DI water, and drying in air.

TiO_2 nanotubular structure

The electrochemical anodisation of the Ti sheet was carried out by using a DC voltage source. Anodic films of TiO_2 nanotubes were grown by potentiostatic anodisation at 20 V using a Pt sheet as a counter electrode in 0.5% hydrofluoric acid solution under stirring conditions at room temperature. The samples were sufficiently rinsed with DI water after anodisation, and calcined at 450°C for 2 hours [19].

TiO_2 sponge-like structure

All the preparation conditions for TiO_2 sponge-like structure were the same as for the above experiments, except the anodising potential was set at 50 V [20].

Nano/micro nest-like TiO_2 structure
The Ti foils were under hydrothermal treatment by 10 M NaOH in the hydrothermal reactor at 150°C for 2 hours. After rinsing sufficiently in DI water, the samples were immersed in 5% HNO_3 solution for 6 hours, rinsed again in DI water, and calcined at 450°C for 2 hours to form anatase [21]. All chemical reagents were from Sinopharm Chemical Reagent Co. Ltd. (Shanghai, China).

Characterisation of surface structure and roughness

The surface morphologies of all the samples were examined using scanning electron microscopy (FESEM, S-4800; Hitachi High-Technologies, Tokyo, Japan). The corresponding crystal structural characterisation was examined using X-ray diffraction (XRD) pattern (X'pert PRO; PANalytical, Almelo, The Netherlands). The XRD patterns were collected in a 2θ range from 20° to 60°. The sessile drop method was used for contact angle measurements with a contact angle meter (OCA-20; DataPhysics, Filderstadt, Germany) at room temperature. A three dimensional (3D) camera optical measurement system (MicroCAD premium, GFM, Berlin, Germany) was applied for average roughness comparison and specific surface area was analysed with a static volumetric method (JW-BK112 Surface Area Analyzer; JWGB Science & Technology Co. Ltd., Beijing, China).

Apatite deposition

The modified simulated body fluid (SBF) was used as an incubation solution for apatite formation. The ion concentrations of SBF are nearly equal to those of the human blood plasma, as shown in Table 1. The SBF recipe was prepared according to the Kokubo's formulation and buffering at pH 7.4 with Tris—hydroxymethyl amino methane and 1.0 M HCl at 37°C. Each sample was placed in a polypropylene tube with 30 mL SBF and kept in an incubator at 37°C for 7 days. To keep the ion concentration stable, the SBF solution was refreshed every 2 days.

In vivo implantation and assay and torque removal force measurement

To test the osteointegration potentials of various surface modifications, medical Ti screws (4 mm diameter × 6 mm length) were subjected to surface modification by the electrochemical means as described above, and four types of screws with the following surface characters were created: (1) nontreatment (blank); (2) TiO_2 nanotubular structure; (3) TiO_2 sponge-like structure; and (4) alkaline hydrothermal treatment with nano/micro nest-like structure. For the implantation, 10 New Zealand white rabbits (male, body weight 3.0—3.5 kg) were used. All the animal studies were carried out following the guidance of the European Commission Directive 86/609/EEC for animal experiments. Under general anaesthesia and sterile conditions, a small incision was made at the medial aspect of the knee joint in both legs to expose the medial proximal tibial plateau and medial distal femoral condyle. A 3.5-mm diameter hole was predrilled and then the testing screw was carefully screwed into position, and the skin was sutured. Each rabbit had four different screws implanted in both femurs and tibiae in a randomly mixed fusion; a total of 10 screws from each group were implanted. All rabbits were terminated at 8 weeks after the implantation and the femurs and tibiae were harvested. All the screws in the femurs ($n = 5$ per group) were used to determine the torque removal force using a manual torque meter (clutch release torque screw driver) according to the manufacturer's instructions (N6-50LTDK; Kanon, Nakamura Company, Tokyo, Japan). The toque force used to unscrew the implanted screws was recorded and compared.

Table 1 Ion concentrations in SBF and human blood plasma.

	Ion concentration (mmol/L)							
	Na^+	K^+	Mg^{2+}	Ca^{2+}	Cl^-	HCO_3^-	HPO_4^{2-}	SO_4^{2-}
Plasma	142.0	5.0	1.5	2.5	103.0	27.0	1.0	0.5
SBF	142.0	5.0	1.5	2.5	147.8	4.2	1.0	0.5

SBF = simulated body fluid.

Histology and radiography examinations

The proximal tibiae with the screws ($n = 5$ per group) were fixed in 10% buffered formalin for 48 hours and processed and embedded in methylmethacrylate (MMA). The infiltration process was carried out by placing the bone specimens into a solution of MMA and dibutylphthalate (3:1) for 48 hours, followed by a further 48 hours in MMA. Embedding of the infiltrated specimens was done in fresh MMA, dibutylphthalate (3:1) and 2.5% benzoyl peroxide solution at 20°C. Polymerisation was completed within 48 hours. Attempts were made to standardise the sectioning at a midsagittal plane of each specimen by cutting the specimen in half (longitudinally in a sagittal plane) using a low-speed diamond saw, and the MMA sections were polished to thin MMA sections (200 μm). For radiographic examination, the thin sections were placed in a sealed chamber inside a high-resolution digital radiography system (Faxitron MX-20 with DC-2 option; Faxitron X-ray Corporation, Lincolnshire, IL, USA), and a digital X-ray was taken with an exposure condition of 24 kV for 3 seconds. For histology examination, MMA resin was removed by immersing the slides in methoxyethyl acetate at room temperature. Slices were taken through graded ethanol and distilled water, stained with Stevenel's Blue, and counter stained with Van Gieson stain, and digital photographs were taken under microscopy and compared.

Statistical analysis

Quantitative data were analyzed using a commercially available statistical program, SPSS version 16 (SPSS Incorporated, Chicago, IL, USA). There were three samples for all studies, except for roughness analyses for Ti substrates and implant torque test that had five samples. Data are reported as mean ± standard deviation. If the difference was determined to be significant after the analysis of

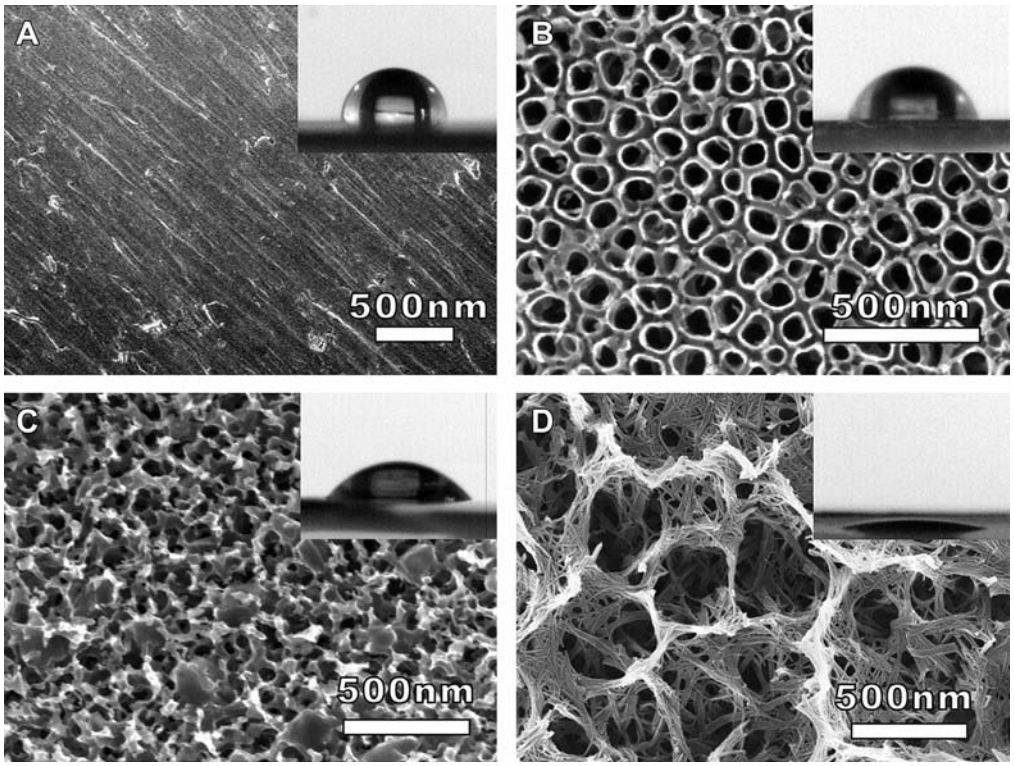

Figure 1 Scanning electron micrographs of the sample surfaces under different treatments. (A) Blank Ti substrate, and corresponding water contact angle (inset). (B) TiO_2 nanotubes (anodising at 20 V), and corresponding water contact angle (inset). (C) Sponge-like structure TiO_2 (anodising at 50 V), and corresponding water contact angle (inset). (D) Nano/micro nest-like structure of TiO_2 prepared by alkaline hydrothermal treatment, and corresponding water contact angle (inset).

variance, pairwise comparisons were performed using a Tukey post-hoc test, and $p < 0.05$ was considered statistically significant.

Results

Surface microstructure

The scanning electron micrographs of the treated surfaces by various techniques are shown in Fig. 1. Fig. 1A represents the mechanically polished Ti surface. Fig. 1B shows the top-view SEM images of the Ti nanotubular structure prepared at 20 V anodisation for 20 minutes. It shows highly ordered nanotube arrays with average inner diameters of 78 nm. Fig. 1C shows that the surface had a uniformly distributed sponge-like nanostructure TiO_2 film treated at 50 V anodisation for 20 minutes. The morphology of Ti surface after alkaline hydrothermal treatment displaced a nano/micro nest-like structure of TiO_2, consisting of uniformed micropores made of nanofibres with average inner diameter of 15—30 nm (Fig. 1D).

Chemical composition

The XRD patterns (Fig. 2) revealed that the treated Ti substrate after annealing had transformed to the anatase phase after either anodisation or hydrothermal treatment. For 50 V anodisation samples, a rutile peak was detected. The stronger and sharper (101 and 200) XRD peaks of TiO_2 coating on nano/micro nest-like TiO_2 structure represented a thicker layer of TiO_2 coating.

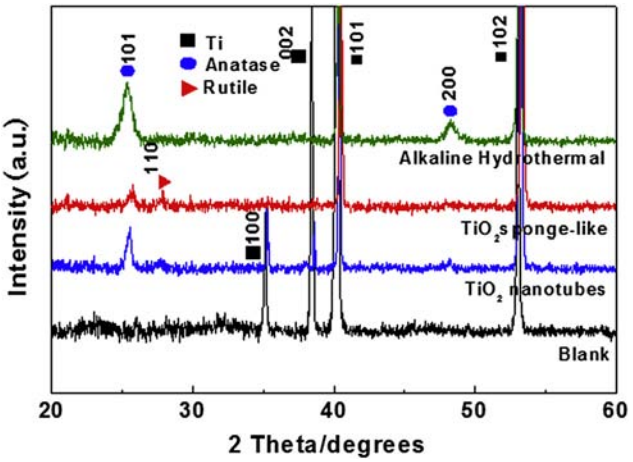

Figure 2 XRD spectra of the oxide film on Ti substrates after different treatments. The XRD patterns revealed that the treated Ti substrate after annealing transformed to the anatase phase after anodisation or hydrothermal treatment. For the 50 V anodisation samples, rutile peak was detected. The stronger and sharper (101 and 200) XRD peaks of TiO_2 coating on nano/micro nest-like TiO_2 structure represent a thicker layer of TiO_2 coating. XRD = X-ray diffraction.

Table 2 Contact angle of different surfaces.

Treatment	Contact angle
Blank	82.3 ± 2.6
TiO_2 nanotubes	70.4 ± 3.4
TiO_2 sponge-like	47.7 ± 6.4
Alkaline hydrothermal	5.92 ± 1.2*

*$p < 0.0001$, compared with the nontreated surface.

Wettability properties

The shape of water droplets on the different treated surfaces is shown as insets in Fig. 1, and the corresponding contact angles are shown in Table 2. The surfaces prepared by anodisation (either at 20 V or 50 V) were slightly hydrophilic compared to blank Ti substrates (Fig. 1A insert) with no significant difference between them (Fig. 1B and C inserts). The contact angle to water for the TiO_2 coating prepared by alkaline hydrothermal treatment was lowest, indicating a super hydrophilic surface (Fig. 1D insert).

Roughness and specific surface area

Table 3 and Fig. 3 exhibit the roughness and specific surface area property data of different surfaces. The rate stands for the ratio against the blank sample value, rate > 1 indicating the increased level of surface roughness and specific surface area. All surface treatments increased the roughness and specific surface area compared to the blank surface, and the increased level of specific surface area was greater than that of the roughness with all surface treatments (Fig. 3).

Apatite-forming behaviour

Fig. 4 shows the surface morphologies of all the samples after soaking in SBF for 7 days. Almost no apatite precipitate was observed on the surface for the untreated blank samples (Fig. 4A) and nanotubular array samples (Fig. 4B). The apatite layer was observed on some parts of nano sponge-like TiO_2 surfaces (Fig. 4C insert). By contrast, a dense and uniform apatite layer that covered all surfaces was seen in the nano nest-like TiO_2 surface, and the apatite layer was thicker than that of the nano sponge-like surface (Fig. 4D).

Implant torque removal force measurement and histological examinations

The removal torque force for the various screws is presented in Table 4. The screws with TiO_2 nanotube structure and alkaline hydrothermal treatment had significantly higher removal torque force compared to the blank (non-treated) screws, and the highest torque force was seen in the TiO_2 nanotube structure group. No difference in the torque force was seen between the TiO_2 sponge-like group and the blank group. The contact soft X-ray and non-decalcified histology examinations revealed integration at the screw bone interface. In the blank and TiO_2 sponge-like group, there was a clear and continuous thin gap between the bony tissues and the screw surfaces, whereas in the TiO_2 nanotube group and the alkaline hydrothermal coating group, the bony tissues were in close or direct contact with the screw surfaces in most parts. Only scattered small gaps (not continuous) visible in the TiO_2 nanotube group and the gap in the alkaline hydrothermal coating group were smaller than that of the TiO_2 nanotube group (Fig. 5).

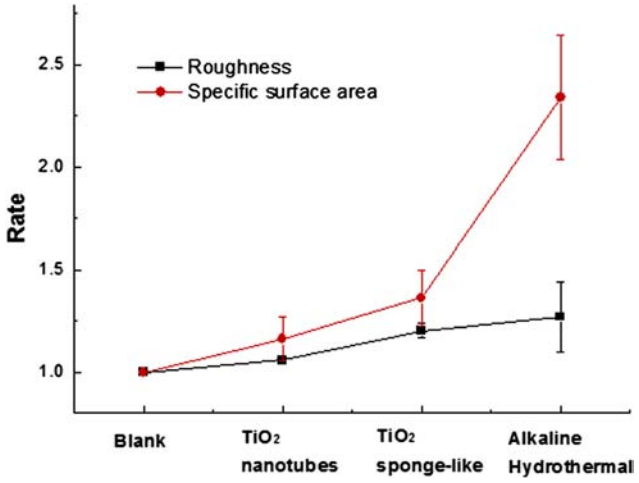

Figure 3 Roughness and surface area increasing rate of different surfaces compared to the blank.

Discussion

It is well known that the surface structures of implants play crucial roles in biocompatibility, bioactivity, and osteointegration of implanted materials. Following implantation, the implant surface immediately interacts with the biological fluids and tissues. The first step in this biological environmental exposure is the rapid adsorption of proteins to the surface of implants, which is largely determined by the implant surface structures. The composition, type, orientation, and conformation of the adsorbed proteins regulate the secondary step, which is cellular attachment and adherence and further proliferation and differentiation. The rate and quality of bone

Table 3 Roughness and surface area data of different samples.

Sample	Roughness (nm)	Rate	Surface area (m^2/g)	Rate
Blank (non-treated)	716.0 ± 14.2	1	3.084 ± 0.630	1
TiO_2 nanotubes	758.7 ± 20.7	1.060 ± 0.008	4.060 ± 0.351	1.316 ± 0.109
TiO_2 sponge-like	861.3 ± 39.6	1.203 ± 0.035	4.739 ± 0.503	1.536 ± 0.137
Alkaline hydrothermal	911.3 ± 33.8	1.273 ± 0.170	8.260 ± 1.051	2.678 ± 0.304

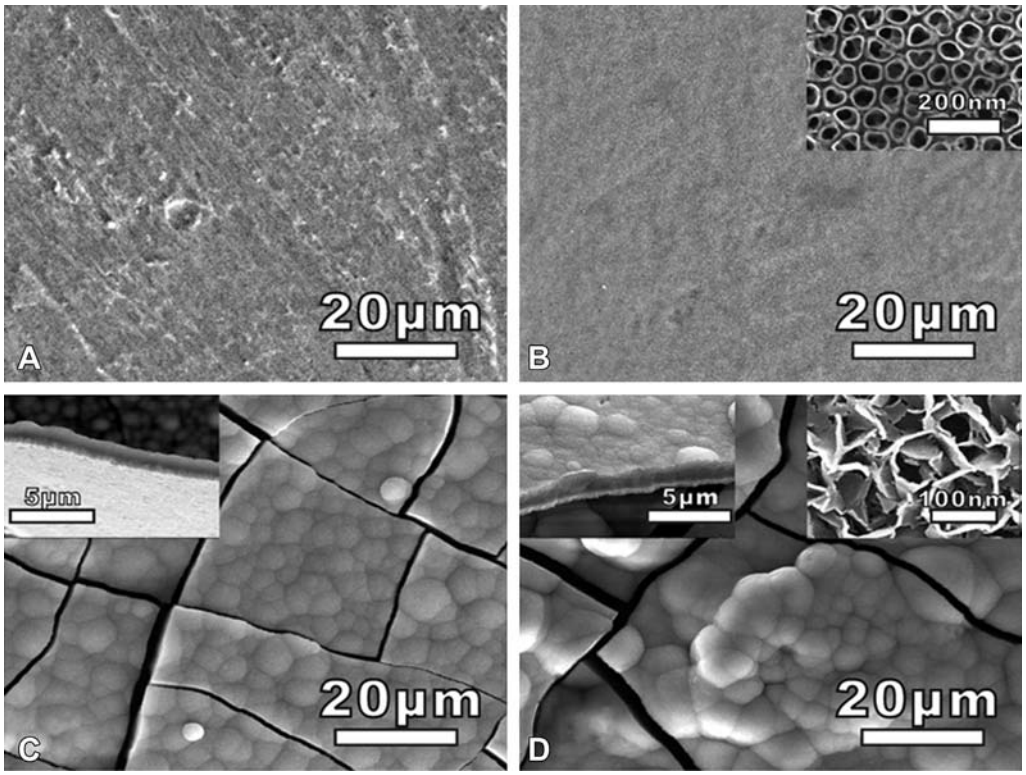

Figure 4 Scanning electron micrographs of different sample surfaces after apatite deposition. (A) Blank Ti substrate. (B) TiO_2 nanotubes (anodising at 20 V), and corresponding higher magnification (inset). (C) Sponge-like structure TiO_2 (anodising at 50 V), and corresponding cross- sectional view (inset). (D) Nano/micro nest-like structure of TiO_2 prepared by alkaline hydrothermal treatment, and corresponding cross-sectional view and higher magnification (inset).

contact with Ti implants are related to their surface structures, such as topography, porosity, dimension, composition, wettability, and surface charge. The design criteria for implant surfaces are: mimic of natural bone surface structures, in nano/microscales with correct chemical composition, wettability, and strong osteointegration ability. In this study, we precisely constructed four different surface structures on Ti surfaces, having: a smooth surface (nontreated); a highly ordered nanotubular arrays with average inner diameters of 78 nm; a sponge-like nano-TiO_2 with lower porosity; and nano/micro nest-like TiO_2 with high porosity. It is noted that the Ti implants with nano/micro nest-like surface structure showed high bone—implant integration, indicating excellent biocompatibility of the nano/micro nest-like surface.

The surface roughness and surface area have profound effects on the bone—implant integration. Recent studies have shown that surface micro-roughness increases osteointegration in the early phases and in areas of low quality bone [19]. Scaffolds with nanoscale architecture have large surface areas to adsorb proteins, which present more binding sites to cell membrane receptors [20]. How cells detect and respond to nanofeatures is not yet fully understood, but it is believed that proteins may "sense" the surface topography at the nanoscale, therefore, materials may be "rough or hostile" to cells with microscale surfaces but "smooth and friendly" with nanoscale surfaces. Our previous work and several studies from other groups have indicated that the nanostructured Ti coating enhances protein polymerization, osteoblast adhesion, or osteointegration [19,22,23], whereas surfaces with rough textures increase the substrate—tissue interlocking and promote osteoblast differentiation [21]. In our study, the nano/micro nest-like TiO_2 surface structure had the greatest roughness and surface area and best bone—implant integration, indicating that alkaline hydrothermal treatment provided a larger surface area to facilitate protein adsorption and cell attachment. The alkaline hydrothermal treatment also produced porosity in both nano- and microscales, and its hierarchical scales may have matched different proteins and promoted cellular adhesion and attachment.

To meet the demands of different phases during the interaction of the cells and implants, comprehensive structural parameters should be considered including chemical composition and hierarchical structure with various dimensions. The nano/micro nest-like surface

Table 4 Removal torque force for various implants.

Materials/surface	Removal torque (N/cm)
Blank (nontreated)	20.3 ± 10.6
TiO_2 nanotube	40.4 ± 6.45*
TiO_2 sponge-like	31.3 ± 5.51
Alkaline hydrothermal	34.3 ± 5.30**

*$p < 0.01$ and **$p < 0.05$, compared to the blank surface.

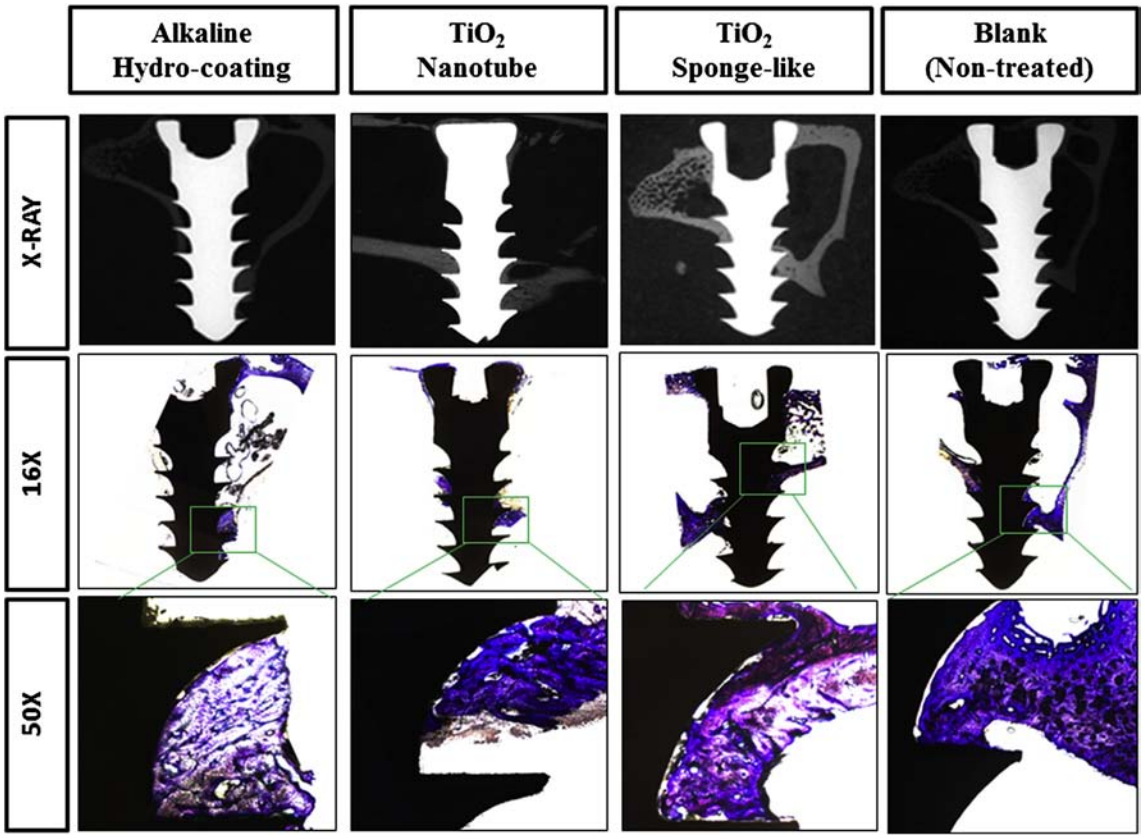

Figure 5 Histological sections of different treated implants 8 weeks after implantation in rabbit femur and tibia showing that the best osteointegration was in the group with nano/micro nest-like structure surface of TiO_2 prepared by alkaline hydrothermal treatment.

exhibited larger specific surface area, suitable roughness, better ability of apatite deposition, and osteointegration *in vivo*, suggesting this construction of nano/micro nest-like surface was able largely to enhance the biocompatibility and osteointegration of the Ti screws. The hierarchical structure in both nano- and microscale pores is beneficial for cellular attachment, proliferation and differentiation. For example, various proteins can "sense" the nano-topography [24]; osteoblasts can spread markedly faster on nanoroughened surfaces and osteoconductivity can be improved [18]. By contrast, the microscale pores on the surface are an excellent match for the platelet adhesion that is considered as the first response after implantation. Platelet aggregation initiates fibrin network formation and assists the adhesion of osteoblasts or other bone-forming cells, and microscale roughness may also improve osteoblast differentiation and growth factor production [25]. The right interfacial microenvironment is crucial for better integration of the implants with surrounding tissues, and the superhydrophilic surface is beneficial to various biological processes, including: protein adsorption; cell adhesion, growth and differentiation; and finally osteointegration. The osteointegration and biomechanical performance of the coated Ti screws were evaluated by histology and removal torque force test *in vivo*. We found that the nano/micro nest-like and nanotube structured surface possessed better osteointegration ability. The torque removal force and histological examination are more direct methods to evaluate the osteointegration of the implant surface compared to *in vitro* cellular examination. There is a strong correlation between the osteointegration of implants with their structural features, chemical composition, and surface properties.

In summary, we successfully fabricated three types of hierarchical structures of TiO_2 coating on Ti implants, including nanotube structure, nano sponge-like structure, and nano/micro nest-like structure, prepared by electrochemical anodisation at 20 V and 50 V, and alkaline hydrothermal reaction, respectively. Our surface-modification strategy, namely to treat the implant surface by alkaline hydrothermal reaction is promising. This method is simple and cost-effective; it does not change the material properties and hence does not need new approval if only surface modification is carried out on the implants. In other words, our product is ready to be tested further in clinical settings. The current study serves as a proof of concept that our surface modification methods may be a novel and better alternative to the existing surface modification products.

Taking all the data together, we found that the alkaline hydrothermally treated Ti substrate was the best for bone—implant integration in terms of all the *in vitro* and *in vivo* testing parameters. The alkaline hydrothermally treated surface displayed hydrophilic wettability, greater roughness, larger specific surface area, and greater apatite inductivity. Electrochemical surface modification may become a powerful approach to enhance metal implant to bone integration in orthopaedic applications.

Conflicts of interest

The authors declare that they have no conflicts of interest.

Acknowledgements

The authors gratefully acknowledge the financial support from the National Natural Science Foundation of China (21021002), the National Scientific Support Program of China (2012BAI07B09), and the Open Project of State Key Laboratory of Physical Chemistry of Solid Surfaces (201205). Financial support from the National Institute of Medical Technology, Beijing, China for the animal purchasing and consumable costs is also acknowledged. In addition, this study was supported in part by SMART program, Lui Che Woo Institute of Innovative Medicine, Faculty of Medicine, The Chinese University of Hong Kong. This research project was made possible by resources donated by Lui Che Woo Foundation Limited.

References

[1] Rupp F, Scheideler L, Olshanska N, De Wild M, Wieland M, Gerstorfer J. Enhancing surface free energy and hydrophilicity through chemical modification of microstructured titanium implant surfaces. J Biomed Mater Res A 2006;76:323—34.
[2] Wennerberg A, Albrektsson T, Andersson B, Krol J. A histomorphometric study of screw-shaped and removal torque titanium implants with three different surface topographies. Clin Oral Implants Res 1995;6:24—30.
[3] Wong M, Eulenberger J, Schenk R, Hunziker E. Effect of surface topology on the osseointegration of implant materials in trabecular bone. J Biomed Mater Res 1995;29:1567—75.
[4] Li D, Ferguson SJ, Beutler T, Cochran DL, Sittig C, Hirt HP. Biomechanical comparison of the sandblasted and acid-etched and the machined and acid-etched titanium surface for dental implants. J Biomed Mater Res 2002;60:325—32.
[5] Cisse O, Savadogo O, Wu M, Yahia LH. Effect of surface treatment of NiTi alloy on its corrosion behavior in Hanks' solution. J Biomed Mater Res 2002;61:339—45.
[6] Chauvy P, Madore C, Landolt D. Variable length scale analysis of surface topography: characterization of titanium surfaces for biomedical applications. Surf Coat Tech 1998;110:48—56.
[7] Wilson A, Leyland A, Matthews A. A comparative study of the influence of plasma treatments, PVD coatings and ion implantation on the tribological performance of Ti—6Al—4V. Surf Coat Tech 1999;114:70—80.
[8] Cordioli G, Majzoub Z, Piattelli A, Scarano A. Removal torque and histomorphometric investigation of 4 different titanium surfaces: an experimental study in the rabbit tibia. Int J Oral Maxillofac Implants 2000;15:668—74.
[9] Larsson C, Thomsen P, Aronsson BO, Rodahl M, Lausmaa J, Kasemo B. Bone response to surface-modified titanium implants: studies on the early tissue response to machined and electropolished implants with different oxide thicknesses. Biomaterials 1996;17:605—16.
[10] Bagno A, Di Bello C. Surface treatments and roughness properties of Ti-based biomaterials. J Mater Sci Mater Med 2004;15:935—49.
[11] Xiao J, Zhou H, Zhao L, Sun Y, Guan S, Liu B. The effect of hierarchical micro/nanosurface titanium implant on osseointegration in ovariectomized sheep. Osteoporos Int 2011;22:1907—13.
[12] Citeau A, Guicheux J, Vinatier C, Layrolle P, Nguyen TP, Pilet P. *In vitro* biological effects of titanium rough surface obtained by calcium phosphate grid blasting. Biomaterials 2005;6:157—65.
[13] Wu Y, Zitelli JP, TenHuisen KS, Yu X, Libera MR. Differential response of staphylococci and osteoblasts to varying titanium surface roughness. Biomaterials 2011;32:951—60.
[14] Al-Nawas B, Groetz K, Goetz H, Duschner H, Wagner W. Comparative histomorphometry and resonance frequency analysis of implants with moderately rough surfaces in a loaded animal model. Clin Oral Implants Res 2008;19:1—8.
[15] Shalabi M, Gortemaker A, Van't Hof M, Jansen JA, Creugers NH. Implant surface roughness and bone healing: a systematic review. J Dent Res 2006;85:496—500.
[16] Dehua L, Stephen JF, Thomas B, David LC, Caroline S, Hans PH, et al. Biomechanical comparison of the sandblasted and acid-etched and the machined and acid-etched titanium surface for dental implants. J Biomed Mater Res 2002;60:325—32.
[17] Gittens RA, McLachlan T, Olivares-Navarrete R, Jansen J, Creugers N. The effects of combined micron-/submicron-scale surface roughness and nanoscale features on cell proliferation and differentiation. Biomaterials 2011;32:3395—403.
[18] Zinger O, Anselme K, Denzer A, Habersetzer P, Habersetzer P, Wieland M, et al. Time-dependent morphology and adhesion of osteoblastic cells on titanium model surfaces featuring scale-resolved topography. Biomaterials 2004;25:2695—711.
[19] Lai YK, Lin CJ, Wang H, Huang JY, Zhuang HF, Sun L. Superhydrophilic—superhydrophobic micropattern on TiO2 nanotube films by photocatalytic lithography. Electrochem Commun 2008;10:387—91.
[20] Yun H, Lin CJ, Li J, Wang JR, Chen HB. Low-temperature hydrothermal formation of a net-like structured TiO2 film and its performance of photogenerated cathode protection. Appl Surf Sci 2008;255:2113—7.
[21] Lai YK, Lin CJ, Huang JY, Zhuang HF, Sun L, Nguyen T. Markedly controllable adhesion of superhydrophobic sponge like nanostructure TiO films. Langmuir 2008;24:3867—73.
[22] Wang H, Lin CJ, Zhao DM, Hu R, Zhang F, Lin LW. A Novel nano-micro structured octacalcium phosphate/protein composite coating on titanium by using an electrochemically-induced deposition. J Biomed Mater Res A 2008;87A:698—705.
[23] Wang H, Lin CJ, Hu R. Effects of structure and composition of the CaP composite coating on apatite formation and bioactivity in simulated body fluid. Appl Surf Sci 2009;255:4074—81.
[24] Kubo K, Tsukimura N, Iwasa F, Ueno T, Saruwatari L, Aita H. Cellular behavior on TiO2 nanonodular structures in a micro-to-nanoscale hierarchy model. Biomaterials 2009;30:5319—29.
[25] Braceras I, Alava J, Goikoetxea L, De Maeztu M, Onate J. Interaction of engineered surfaces with the living world: ion implantation vs. osseointegration. Surf Coat Tech 2007;201:8091—8.